APPLICATION OF HP-FINITE ELEMENT FORMULATION TO NON-LINEAR HEAT CONDUCTION PROBLEMS WITH SOURCE TERMS

Djebar Baroudi

Rakenteiden Mekaniikka, Vol. 29
Nro 3-4, 1996, s. 75-86

ABSTRACT

This work presents an application of the hp- finite element formulation to solve the general non-linear heat conduction problem in a solid for cases involving heat sources and non-linear boundary conditions terms. The temperature field is semi-discretized in space with hierarchical basis functions formed using the orthogonal Legendre polynomials. The good approximation properties of the hp-finite element method are achieved here by the combined effect of the traditional mesh refinement together with the p-extension of the polynomial basis. Because the temperature field is continuous, the hp-formulation performs very well. The calculated temperature field converges much faster in the hp-version than the traditional h-refinement. In general, the h-refinement is used for regions with non-smooth solution and the p-extension for the smooth ones. This work also shows a systematic way to treat source terms and the possible non-linear natural boundary conditions present in the heat conduction equation by including them in the force vector of the discretized heat conduction equation.

NOMENCLATURE

c	specific heat, J/(kg K)
e	superscript for the element number e
$\mathbf{f}$	force vectors
q	heat flux, W/m^2
r	heat generation rate per unit volume, W/m^3
t	time, s
x	space dimension, m

w_K	weights of the Gauss-integration points
$\mathbf{C}$	capacitance matrix
$\mathbf{K}$	conductance matrix
L	latent heat per unit mass, J/kg
N_i	shape functions
P_i	Legendre polynomials
$\mathbf{T}$	degrees of freedom, temperatures, K
λ	thermal conductivity, W/(m K)
v	test function
ρ	density, kg/m^3
ξ_K	co-ordinates of the Gauss-integration points

INTRODUCTION

Heat conduction problems are of importance in many engineering fields. Heat generation occurs in many situations dealing with chemically or biologically active materials, such as cellulose, wool or coal. Even insulation materials such, as mineral wool, may generate heat due to the exothermic reactions of the binder. In most cases, the rate of internal heating is temperature dependent. In some cases, the internal heat generation can lead to what is called self-ignition without any heat from the outside. Self-ignition may appear when, for instance, considerable amounts of materials are kept together and/or moisture content reaches some critical level. Good examples of that are storage silos and storage problems [1] and [2].

Pham [3] and [4] suggested that the internal heating can be treated as a special form of specific heat. In the present paper, a different approach is taken. First, heat generation terms are treated as simple source terms. All the non-linear source terms, together with the possible non-linear natural boundary conditions - convection/radiation - are systematically included in the force vector of the discretized heat conduction equation. This non-linear system of equations is then solved using an iterative method with the fixed point algorithm at each time step. This allows us to treat any source terms in a clear and systematic way. The *hp*-semi-discretization is used to accelerate the convergence of the solution with respect to the space variable [5, IV] and [6]. Thus, the number of unknowns is significantly reduced compared to the classical *h*-version where the same result is achieved by a finer refinement of the geometrical mesh, which usually means that much more degrees of freedom are needed. This procedure is shown using examples from the 1-D problems. This can be extended to 2-D without any loss of generality [5, VI].

Standard Galerkin finite element formulation is applied where the space is discretized using a traditional geometrical h -mesh and the basis functions are the hierarchical basis functions formed using the orthogonal Legendre polynomials, see [5, III] and [6]. For shortness, by convergence we mean here the convergence with respect to the space dimension not the time dimension. It is presumed that the time-integration method is a convergent one. By h-refinement we mean that the convergence of the numerical solution to the analytical one is achieved by the refinement of the geometrical mesh. By p-extension we mean that convergence is achieved by extending the dimension of the orthogonal basis function set $\{N_1, N_2, N_3, \dots, N_{p-1}, N_p\}$, i.e. increasing the degree p of the polynomials. The first two shape functions $\{N_1, N_2\}$ are the usual linear basis functions, while the remaining part $\{N_3, \dots, N_{p-1}, N_p\}$ is formed with the Legendre polynomials. The functions of the last set are also called bubble functions. An optimal convergence rate is achieved when using hp-version, i.e. the combined effect of the traditional mesh refinement together with the p-extension of the polynomial basis. In this case, the h-refinement is effective for regions with non-smooth solution and the p-extension for the smooth ones. The degree of the polynomials can be increased without any problems in numerical stability because the Legendre polynomials are orthogonal. The non-linear global semi-discrete system of ODE are time-integrated using a first order Backward-Euler scheme associated with the fixed point iteration procedure at each time step to solve the resulting system of coupled non-linear equations [7, XVIII, XX and XXI] and [8, VIII]. Besides the usual possible material nonlinearity, the non-linearity in boundary conditions and source terms is present.

Comparison of analytical and numerical calculations is also shown.

FORMULATION OF THE PROBLEM

The basic idea is to solve the temperature field $T(x,t)$ in a given material region. The field equation

$$\rho(T)c(T)\frac{\partial T(x,t)}{\partial x}=\frac{\partial}{\partial x}\left(\lambda(T)\frac{\partial T(x,t)}{\partial x}\right)+r(x,T) \quad (1)$$

is the diffusion equation with $r(x,T)$ as an arbitrary source term. The 1-D case is only for simplicity and to illustrate the process. The Fourier heat conduction constitutive relation is assumed. This equation is complemented with the appropriate initial-boundary conditions to get a well-posed problem. The boundary conditions may be a Direchlet type or Neumann type, for instance, normal heat flux $q_n = h(T)(T-T_\infty)+\sigma\varepsilon(T^4-T_\infty^4)$ with convection and radiation parts. The boundary terms as well as the source terms if present will be included in the force vector of the discretized heat conduction equations. This will be a clear and systematic way to treat boundary and source terms. Source terms may be arbitrarily given. Usually one may see, for example, an Arrhenius type dependence $r(x,T)=Q_0(x,T)\cdot\exp(-E/(RT(x)))$. This kind of behaviour is exibited by a number of 'materials' encountered in practice.

SEMI-DISCRETIZATION OF THE FIELD EQUATIONS

Using the standard Galerkin method [7] and [8] one obtains the variational form of the problem (1) as

$$\int_0^L \rho c\frac{\partial T}{\partial t}v\,dx+\int_0^L \lambda\frac{\partial T}{\partial x}\frac{\partial v}{\partial x}dx=\int_0^L rv\,dx-\left[q_{con}v\right]_0^L \quad (2)$$

with the temperature field approximated by $T^e(x,t)=\mathbf{N}^e(x)\mathbf{T}^e(t)$, where the test and the basis functions are

$$N_1(\xi)=\frac{1-\xi}{2},\; N_2(\xi)=\frac{1+\xi}{2} \text{ and } N_i(\xi)=\frac{1}{\sqrt{4i-6}}(P_{i-1}(\xi)-P_{i-3}(\xi)), \quad i=3,4,... \quad (3)$$

The Legendre polynomials $P_i(\xi)$ are defined by the recursion [5]:

$$P_0(\xi)=1,\quad P_1(\xi)=\xi,\quad P_2(\xi)=\frac{1}{2}(3\xi^2-1),...,(m+1)P_{m+1}(\xi)=(2m+1)P_m(\xi)\xi-mP_{m-1}(\xi), m=1,2,... \quad (4)$$

The Legendre polynomials are orthogonal in the sense that $\int_{-1}^{+1}P_i(\xi)P_j(\xi)d\xi=2/(2i+1)$ for $i=j$ and equal to zero for $i\neq j$. The orthogonality will give a numerically stable method when extending the polynomial basis $\{N_1, N_2, N_3, \dots, N_{p-1}, N_p\}$ by increasing the degree p of the polynomials.

The semi-discretization of the heat conduction equation (1) produces the non-linear initial value problem

$$\mathbf{K}(t,\mathbf{T})\mathbf{T}(t)+\mathbf{C}(t,\mathbf{T})\dot{\mathbf{T}}(t)=\mathbf{f}(t,\mathbf{T}), \quad t>0 \tag{5.1}$$

$$\mathbf{T}(0)=\overline{\mathbf{T}}_0, \quad t=0 \tag{5.2}$$

where $\mathbf{T}(t)=\begin{pmatrix}T_1(t) & T_2(t) & \dots & T_m(t) & T_{m+1}(t) & \dots & T_n(t)\end{pmatrix}^T$ is the global vector of degrees of freedom. In the vector of the unknowns, the first terms $1 \dots m$ are the nodal temperatures while the remaining $m\text{-}1 \dots n$ represent the coefficients of the corresponding bubble functions N_i, $i > 2$. The spatial discretization - h-mesh - is performed with 2-node elements of arbitrary lengths giving the geometrical mesh consisting of nodes globally numbered as $1, \dots, (i\text{-}1), (i\text{+}1), \dots, (m\text{-}1), m$.

Equation (5.1) is an ordinary $n \times 1$-differential nonlinear equation. Notice that the right hand in equation (2) corresponds to the force vector $\mathbf{f}(t,\mathbf{T})$, which contains the boundary terms, as also all possible source terms. Equation (5.1) is be complemented with appropriate initial conditions (5.2). Natural boundary conditions are already included in the variational form (2). The essential boundary conditions will be taken into account during the solution process of the intial value problem. The global matrices and vectors are assembled using standard FE-assembling techniques as

$$\mathbf{K}(t,\mathbf{T})=\sum_{e=1}^{N^e}\mathbf{L}^{eT}\mathbf{K}^e(t,\mathbf{T}^e)\mathbf{L}^e, \quad \mathbf{C}(t,\mathbf{T})=\sum_{e=1}^{N^e}\mathbf{L}^{eT}\mathbf{C}^e(t,\mathbf{T}^e)\mathbf{L}^e \quad \text{and} \quad \mathbf{f}(t,\mathbf{T})=\sum_{e=1}^{N^e}\mathbf{L}^{eT}\mathbf{f}^e(t,\mathbf{T}^e) \tag{6}$$

where the elementary connectivity matrices $\mathbf{L}^e$ are such that the local degrees of freedom $\mathbf{T}^e$ are expressed in the global degrees of freedom $\mathbf{T}$ as $\mathbf{T}^e(t)=\mathbf{L}^e\mathbf{T}(t)$. The supscript e points to elementary matrices or vectors: the conductivity matrix

$$K_{ij}^e=\frac{2}{l^e}\int_{-1}^{1}\lambda(T(\xi))\frac{\partial N_i(\xi)}{\partial \xi}\frac{\partial N_j(\xi)}{\partial \xi}d\xi, \tag{7}$$

the capacity matrix

$$C_{ij}^e = \frac{l^e}{2}\int_{-1}^{1} \rho(T(\xi))c(T(\xi))N_i(\xi)N_j(\xi)\, d\xi \text{ ja} \tag{8}$$

and the force vector

$$f_i^e = \frac{l^e}{2}\int_{-1}^{+1} r(T(\xi))N_i(\xi)\, d\xi - \left[q_n N_i(\xi)\right]_{-1}^{+1} \tag{9}$$

are integrated numerically using a Gauss-Legendre integration scheme with as many integration points as needed to integrate their expressions accurately. For example, the contribution of the source term to the force vector source term is space-integrated as $f_{r,i}^e \approx \frac{2}{l^e}\sum_{K=1}^{NG} r(T(\xi_K))N_i(\xi_K)w(\xi_K)$. The elementary matrices and vectors may depend on the unknown temperature.

TIME-INTEGRATION OF THE ODE-SYSTEM

The non-linear initial value problem (5) is then time-integrated by a first order A-stable Backward-Euler. Here the time derivative is approximated by the first term of the Taylor series development

$$\dot{\mathbf{T}}(t_n) = \frac{\mathbf{T}(t_n) - \mathbf{T}(t_{n-1})}{\Delta t_n} + O(\Delta t_n^2). \tag{10}$$

The time-integration gives us the nonlinear system of equations

$$\mathbf{A}(t_n, \mathbf{T}_n)\mathbf{T}(t_n) - \mathbf{g}(t_n, \mathbf{T}_n) = \mathbf{0} \tag{11}$$

for which the solution **T**(t) is solved from equation (10) at each time step using the fixed point iteration procedure. The matrix in equation (11) is calculated as

$$\mathbf{A}(t_n, \mathbf{T}_n) = \mathbf{C}(t_n, \mathbf{T}_n) + \Delta t_n \mathbf{K}(t_n, \mathbf{T}_n) \tag{12}$$

and the vector

$$\mathbf{g}(t_n, \mathbf{T}_n) = \mathbf{C}(t_n, \mathbf{T}_n)\mathbf{T}(t_{n-1}) + \Delta t_n \mathbf{f}(t_n, \mathbf{T}_n). \tag{13}$$

At a given time t_n, the system (11) is solved iteratively by the fixed point algorithm. Matrices and vectors are updated inside each iteration step j for each time step n. The fixed point iteration scheme starts from known initial conditions. Beginning from a known value (known from the previous iteration number j) of the temperatures $\mathbf{T}^j_n$. Then from equation (11) one gets an improved estimate $\mathbf{T}_n^{j+1}$ at the $j+1$:th Picard iteration. This iteration procedure is repeated for t_n until convergence is reached, i.e., $\|\mathbf{T}_n^{j+1} - \mathbf{T}_n^j\|_2 \to 0$. After this we move to the next time step t_{n+1} and repeat the procedure. In this way a solution $\mathbf{T}(t)$ is constructed, and using equation $T(x,t) = \mathbf{N}(x)\,\mathbf{T}(t)$ all the temperature field is obtained.

NUMERICAL EXAMPLES

Test problem 1

Heat generation with linear temperature dependence. The example consists of a slab of unit length initially at a constant temperature $T_0(x) = 0$ with surface $x = 1$ maintained at zero temperature. At $x = 1$ there is no flow of heat, i.e. adiabatic boundary condition. The heat production rate is $r(x,T) = T + 1$. The analytical solution of this example is presented by Carslaw and Jaeger [9, XV, pp. 404].

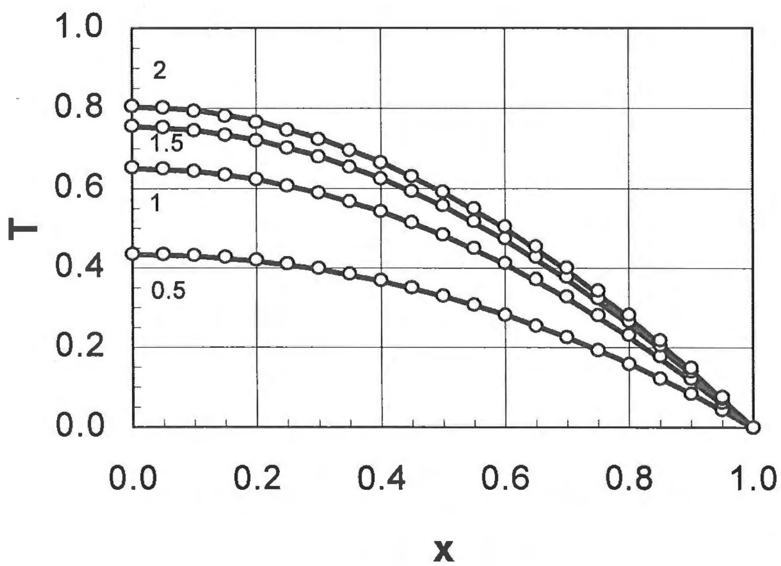

Figure 1. Numerical and analytical solutions. Markers show numerical solution. Continuous line shows the analytical solution from Carslaw and Jaeger at different time steps 0.5, 1, 1.5 and 2 s.

All other material properties are set to unity. The time step used in the numerical integration was 10^{-4} s. The space mesh consists of two elements of equal length $h = 0.5$, i.e. three nodes. The local shape functions used were $\{N_1, N_2, N_3\}$ giving a total of five degrees of freedom. In other words, one parabolic bubble function N_3 and two linear $\{N_1, N_2\}$ basis functions are used. If compared to the h-version - refinement of the geometrical mesh and using as a set of basis functions the set $\{N_1, N_2\}$ - one way needs much more degrees of freedom to achieve the same accuracy level.

Figure 1 shows the analytical solution as a thick line compared with its numerical solution shown with the markers. The numerical solution is plotted at each 0.05 unit step for clarity in the chart. The numerical solution converges practically very well to the analytical solution with only five degrees of freedom. Thus, this hp-approach seems to perform well. Notice how efficiently the temperature profile is captured with only a total of five degrees of freedom.

Test problem 2

The second example treated is heat generation with linear temperature dependence. This example is the same as in test problem 1 with the only difference in the natural boundary condition. At $x = 1$ a convection boundary condition is set with a convection coefficient equal to unity. The analytical solution of this problem is presented by Carslaw and Jaeger [9, XV, pp. 405] and Pham [3].

The time step used in the numerical integration was 10^{-4} s. The space mesh consists of only one element of length $h = 1$, i.e. two nodes. The local shape functions used were $\{N_1, N_2, N_3\}$ giving a total of three degrees of freedom. Therefore, as below also two linear $\{N_1, N_2\}$ and a parabolic bubble function N_3 are used.

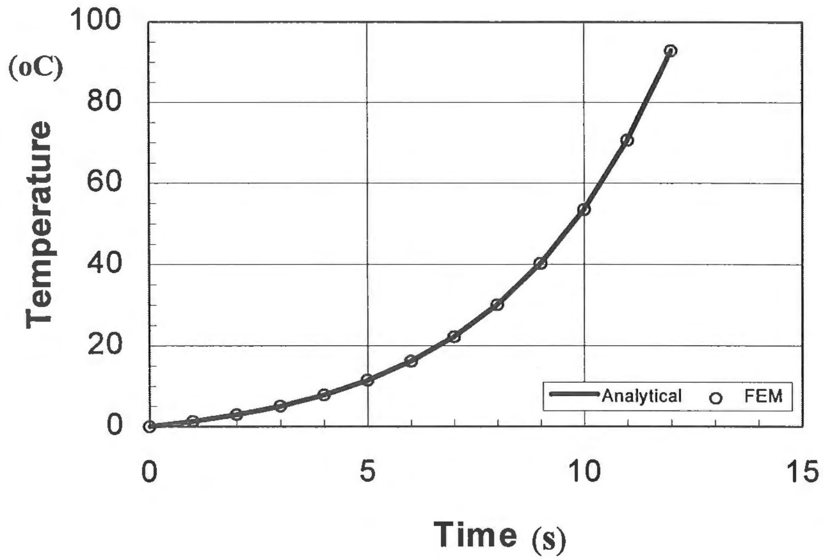

Figure 2. Numerical and analytical solutions as a function of time. Markers show numerical solution. Continuous line shows the analytical solution from ref. [3] at the position x = 0.

Figure 2 shows the good agreements between the analytical solution, the thick line, compared to its numerical solution. A 'minimal' number of degrees of freedom were used, here only a total of three.

Test problem 3

Arrehenius type heat generation. A third example which is in fact a 1-D variation of the example presented in Pham [3]. Pham et al. report ignition tests [10] on cubes of rice husks. The sample treated in the current calculation consists of thickness $d = 8\ cm$ slab of rice husks with two other dimensions assumed much more larger than the thickness. Depending on certain conditions, this biological material may undergo exothermic reactions whose heat production rate follows the Arrhenius rate equation in the form $r(x,T) = Q_0(x,T)\cdot \exp\left(-E/\left(RT(x)\right)\right)$.

This example is computed using the material properties presented in ref. [3] The material properties are: conductivity λ = 0.0951 W/m K, ρc = 28500 J/kg K, ρQ_0 = 2.247 x 10^{15} W/m^3 and E/R = 12560 K. In the calculation a density of unity was used. The initial temperature of the slab was spatially constant and equal to 5 ^{o}C. The boundary conditions at $x = 0$ and at $x = d$ are the normal component - to the surface of the slab - of the combined convection-radiation heat flux vector $\vec{q} = h(T_s)(T_s - T_\infty)\vec{i} + \sigma\varepsilon(T_s^4 - T_\infty^4)\vec{i}$ with a convection coefficient of 5 W/m^2 K and an emissivity of 0.7. The surface temperature of the slabe is T_s. The slab initially at the initial temperature is suddenly submitted to an ambient temperature T_∞. With this example we want to show an application for which the source term - Arrhenius term - and the boundary term - nonlinear convection-radiation term - are simply and systematically treated by including them in the force vector of the discretized heat conduction equation.

In case a) the ambiant temperature was 155 ^{o}C. This case leads to no self-ignition, see Figure 3a. If the ambient temperature is now 165 ^{o}C - case b) - one can see, Figure 3, that thermal instability occurs. Pham in ref. [3] found that the self-ignition for a cube of 8 cm side occurs at an ambient temperature somewhere between 160 ^{o}C and 165 ^{o}C. For the 8 cm thick slab, an analogical result is achieved when the critical ambient temperature is between 155 C and 165 ^{o}C. It was not our goal here to get a sharper estimate for the critical ambient temperature but rather to get a qualitatively satisfactory agreement between observations and calculations.

In the numerical calculation performed the geometrical mesh consists of only one 2-node h-mesh of length h = 8 cm. The local shape functions used were $\{N_1, N_2, N_3\}$ giving a total number of only three degrees of freedom. The time step used for case a) was 0.1 s. For the case b) the time step was varying between 0.0001 s and 0.1 s.

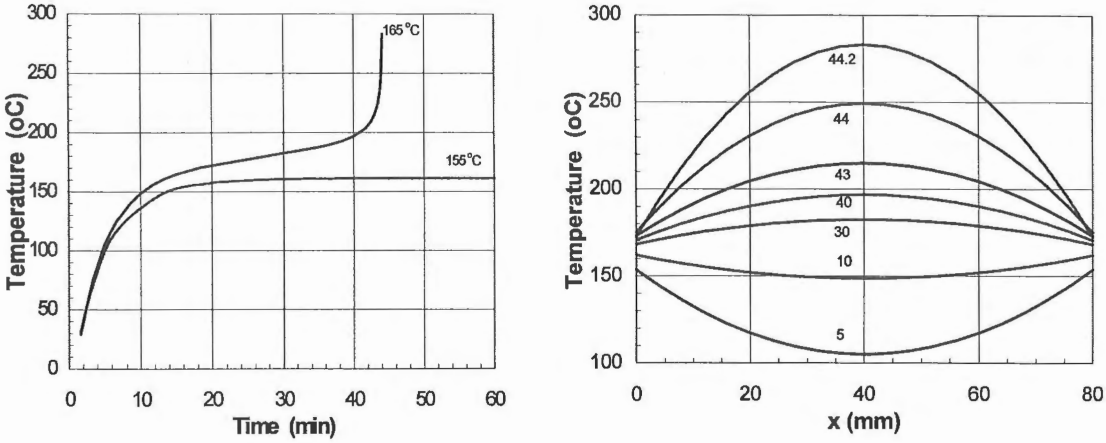

Figure 3. Numerical solution for the temperature at the middle of the slab as a function of time a) for ambient temperature of 155 °C and 165 °C. b) Calculated temperature profiles in the slab at different times for the case of ambient temperature of 165 °C.

Figure 3 shows the agreement between the analytical solution and the expected behaviour. Observe that the temperature profile is well captured by using only one element and one bubble function N_3 in addition to the usual two linear shape functions N_1 and N_2, i.e. only three degrees of freedom.

CONCLUSION

Problems with temperature dependent heat generation and non-linear boundary conditions are treated systematically by including these terms in the force vector of the discretized heat conduction equation. Other methods exist where, for instance, the source terms are treated as changes in the specific heat of the material. The approach presented here is clear and systematic. By using the *hp*-formulation less degrees of freedom are needed compared to the traditional *h*-version to achieve results of a similar accuracy. The good approximation properties of the *hp*- finite element method are achieved here by the combined effect of the traditional mesh refinement together with the *p*-extension of the polynomial basis. Since the temperature field is continuous, the *hp*-formulation is effective. The calculated temperature field converges faster in the *hp*-version than in the traditional *h*-refinement. In general, in the *hp*-version, the *h*-refinement is used for regions with non-smooth solution and the *p*-extensions for the smooth ones. The presented application can be easily extended to 2-D by choosing appropriate elements and appropriate basis function set.

REFERENCES

[1] Dougal Drysdale. An Introduction to Fire Dynamics, *John Wiley and Sons, New York 1986*, pp. 424.

[2] B. F. Gray, J. F. Griffiths, and S. M. Hasko, Spontaneous Ignition Hazards in Stockpiles of Cellulosic Materials: Criteria for Safe Storage, *J. Chem. Technol. Biotechnol., vol. 34A, pp. 453-463, 1984.*

[3] Q. T. Pham, Finite Element Procedure for heat conduction problem with internal heating, *Numerical Heat Transfer, Part A, 27:611, 1995.*

[4] Q. T. Pham, A Numerical Scheme for Heat Conduction Problems with Internal Heating, *Proc. Chemica 92, vol. 2, pp. 337-344, 1992.*

[5] B. SZABO, I. Babuška. Finite Element Analysis, *John Wiley & Sons, 1991*, pp. 357.

[6] IVO Babuška and Manil Suri, The p and h-p versions of the Finite Element Method, Basic Principles and Properties, *SIAM Review, Vol. 36, No. 4, pp.578-632, December 1994.*

[7] O. C. Zienkiewicz, FRS. The Finite Element Method in Engineering Science, 3rd Edition, *Mc Graw-Hill, Berkshire, England 1986*, pp. 787.

[8] C. Johnson. Numerical Solutions of Partial Differential Equations by the Finite Element Method, *Studentlitteratur, Lund, Sweden*, 1987, pp. 278.

[9] H. S. Carslaw and J. C. Jaeger. Conduction of heat in solids. *Oxford 1959, Oxford University Press*. pp. 282-296.

[10] Q. T. Pham, I. R. Brown, and J. C. Jones, Combustion Reactivity of Rice Husks: An Experimental and Numerical Investigation, *J. Thermal Sci., vol. 2, pp. 152-156, 1993.*

Djebar Baroudi, MSc Tech

VTT Building Technology

Fire Technology

P.O. Box 1803, FIN-02044 VTT, Finland

Internet: Djebar@Baroudi.vtt.fi